Patterning of worm-like soft polydimethylsiloxane structures using a TiO_2 nanotubular array

Harito, Christian; Lledo, Rosa C.; Bavykin, Dmitry V.; Moshrefi-Torbati, Mohamed; Islam, Aminul; Yuliarto, Brian; Walsh, Frank C.

Published in:
Journal of Applied Polymer Science

Link to article, DOI:
10.1002/app.49795

Publication date:
2020

Document Version
Peer reviewed version

Patterning of worm-like soft polydimethylsiloxane structures using a TiO_2 nanotubular array

Christian Harito[1,2,*], Rosa C. Lledo[3,4], Dmitry V. Bavykin[5], Mohamed Moshrefi-Torbati[3], Aminul Islam[4], B. Yuliarto[6,7], Frank C. Walsh[5]

[1] Department for Management of Science and Technology Development, Ton Duc Thang University, Ho Chi Minh City, Vietnam.

[2] Faculty of Applied Sciences, Ton Duc Thang University, Ho Chi Minh City, Vietnam.

[3] Mechatronics Research Group, University of Southampton, Southampton SO17 1BJ, United Kingdom.

[4] Department for Mechanical Engineering, Technical University of Denmark, Kongens Lyngby, 2800, Denmark

[5] Energy Technology Group, University of Southampton, Southampton SO17 1BJ, United Kingdom.

[6] Advanced Functional Materials (AFM) Laboratory, Engineering Physics, Institut Teknologi Bandung, 40132, Bandung, Indonesia.

[7] Research Center for Nanosciences and Nanotechnology (RCNN), Institut Teknologi Bandung, 40132, Bandung, Indonesia.

*Email: christianharito@tdtu.edu.vn

KEYWORDS anodising; moulding; PDMS; soft lithography; TiO_2 nanotubes.

ABSTRACT: Patterned polydimethylsiloxane (PDMS) is an important structure for soft lithography. Various natural and synthetic materials have been deployed as mould for patterning PDMS. Anodised nanotubular array has been sought after as cost-effective alternative for textured silicon. An array of TiO_2 nanotubes with characteristic diameter ≈140 nm and the length of ≈1.5 microns, created by anodic oxidation of titanium substrate, was used here as a template for soft PDMS moulding. The optimal moulding process was developed by a combination of silanisation, use of solvent, application of a vacuum, and hydraulic pressing. The silanisation was confirmed by Fourier transform infrared spectroscopy and contact angle measurement while the PDMS structure was examined by scanning electron microscope and energy dispersive X-ray spectroscopy. Hydraulic pressing significantly improved the infiltration of PDMS into the pores of nanotubular array resulting in formation of PDMS nano-bumps after separation of the polymer from the template. Complete infiltration of PDMS precursor into the cavity of nanotubes was observed on the hydraulic-pressed sample without toluene impurities. The hydraulic-pressed samples exhibited higher adhesion strength compared to non-pressed ones. The adhesive strength was measured by simple experimental setup, in which the PDMS was stuck on glass surface vertically followed by pulling it down.

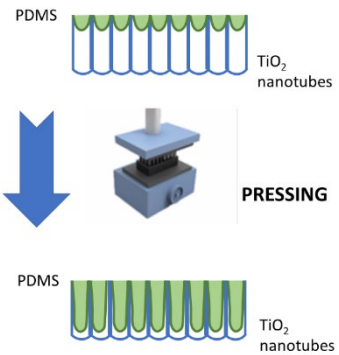

Graphical Abstract

1. Introduction

Soft lithography, an alternative method of photolithography, provides low cost and rapid fabrication of micro- and nanostructures by eliminating the needs of high radiation equipment [1]. Such nanofabrication technique is rapidly advancing many areas of research such as tissue engineering [2], protein printing [3], anti-biofouling [4], dry adhesive [5], and microfluidic [6]. The process begins with fabrication of patterned mould or stamp which is deployed to replicate the micro- or nanostructure. Polydimethylsiloxane (PDMS) is often used as an elastomeric stamp or mould due to its low shrinkage rate [7], hence the name "soft" in soft lithography. The stamp or mould with patterned structure is a key aspect to prototype micro- and nanostructure [8]. The patterned surface has numerous potentials in microelectronics and life sciences. In microelectronics, patterned PDMS is usually used as stamp to fabricate thin film of semiconductor, metal, or insulating materials for microelectronic devices [9]. In life sciences, textured PDMS is often utilised as substrate for microfluidic devices especially for studying the cell adhesion and protein adsorption [10]. It also can be used as dry electrode sensor patch in wearable sensor [11]. Therefore, the development of an elastomeric stamp or mould on a submicron or nano size is crucial.

A PDMS stamp can be achieved either by masking the flat PDMS followed by etching with ultraviolet (UV) light [12], or by moulding of PDMS using textured surfaces from natural or synthetic materials. Natural materials such as plant leaves [13–15], shark skin [16], and sea urchin [17] have micro-patterned surface that can be deployed for PDMS mould. Geometrically complex surfaces from nature may provide the opportunity to enhance understanding of microbial attachment on a unique topography. However, the low stability of the natural products prevents high curing temperature of PDMS which may alter the surface texture of

the natural mould. Low curing temperature (40-80^{o}C) is usually used for natural mould yielding relatively low elastic modulus of PDMS even at a longer curing time. For high curing temperature, synthetic materials such as micro/nanofabricated silicon [18,19] , SU-8 epoxy [20], CuO nanowire [21] porous nickel oxide [22], and alumina nanotubes array [23–25] can be utilised.

Photolithography is needed to synthesise patterned silicon, SU-8 epoxy, and CuO nanowire while a relatively simpler and cost-effective technique such as anodising and electrodeposition can be used for ceramic microfabrication. Nickel particles were electrodeposited from a nickel chloride aqueous electrolyte (pH 4) on the stainless steel cathode using a DC power supply (3 A) [22]. Hydrogen gas evolution at the cathode resulted in pore formation in the nickel layer. The deposited nickel particles mutually coalesced on sintering at 600–800^{o}C while larger pores left cavities (5 µm in diameter) in the film. An uncured PDMS mixture was poured into the cavities, cured and peeled from nickel film creating microfabricated PDMS pillared film with 3-5 µm in diameter and 5–10 µm in length.

Anodic aluminium oxide (AAO) nanotubes template with a diameter of 25–300 nm was attainable by controlled anodising of aluminium in presence of fluoride ions [26]. Instead of negative replica of nanotubes (e.g., pillars, fibres), cone shaped bumps with a diameter of ≈100 nm were fabricated by moulding soft PDMS (Sylgard 184) into 100–200 nm anodised aluminium oxide (AAO) nanotubes [23,24]. When using aluminium as a substrate for the aluminium oxide layer, the heating rate required carefully control to avoid crack formation between aluminium and aluminium oxide, since the coefficient thermal expansion (CTE) of aluminium and aluminium oxide are 13.1×10^{-6} °F^{-1} and 4.5×10^{-6} °F^{-1} [27]. The CTE of titanium and titania are 8.41×10^{-6} °C^{-1} and 9×10^{-6} °C^{-1} hence titanium has less thermal mismatch and is suitable for heating [27]. Moreover, silanised titania shows interchangeable surface wetting

from hydrophobic to hydrophilic on UV irradiation [28] and annealing [29] providing a versatile surface for moulding polymers.

An accurate replica of soft PDMS with high aspect ratio and good quality using a pores smaller than 150 nm is still challenging task [19]. A higher fidelity of PDMS at smaller diameter (≈100 nm) was produced on the silicon template, with composites of two different PDMS layers [30]. A stiffer polymer consisting of vinyl and hydro silane end-linked polymers (hard PDMS, h-PDMS) was used as the first layer which improved the quality of the replica due to its lower viscosity. Whilst soft PDMS was deployed as second layer to give a flexible support of PDMS composite film. However, only nanobumps of soft PDMS with the height of ≈25 nm and ≈80 nm in diameter were observed in a high density AAO nanotube array [25].

Anodising is a relatively simple and cost-effective method which is promising for lithography. To the best of our knowledge, only soft PDMS bumps with low aspect ratio (<2) were produced by replicating anodised sample [23–25]. An intensive research is needed to improve the aspect ratio of PDMS replica. In this work, the facile approach of anodising was used to fabricate a titanium oxide or titania nanotubular template. Titania can be produced in controlled morphologies, including nanotubes, nanofibres, and nanosheets [31,32]. Grimes *et al.* [33] introduced the first generation of titania nanotubes with a length up to 500 nm by anodising in hydrofluoric acid (HF) aqueous solution. During anodising, titania nanotubes were also simultaneously etched by the acid, limiting the length of nanotubes. As an alternative, non-aqueous solutions (e.g., glycerol, ethylene glycol) containing fluoride ions can be used as electrolyte [34,35]. The limited solubility of titanium fluoride in ethylene glycol-based electrolytes manifested a high aspect ratio and ultra-long nanotubes up to 720 µm which comparable to hard anodising of aluminium. Whereas a more viscous solution, such

as glycerol exhibited moderate growth rate up to 7 µm for 13 h. Here, environmentally friendly glycerol was used to produce a considerable nanotubes length. Water content and applied voltage may improve the tubes diameter and length while duration of anodising affects the length [36]. However, water may distort the shape of the ordered tubes array, so the water content was kept at 2 vol.% in this work.

Patterned PDMS was produced using only one layer of soft PDMS (Sylgard 182) for simplicity. Sylgard 182 is similar to Sylgard 184 with a longer working time at 25^{o}C [37] allowing more time for PDMS to fill the pores of the template. An optimal moulding process was achieved by a combination of silanisation, the use of solvent, the application of a vacuum, controlled peeling rate, and hydraulic pressing. The importance of hydraulic pressing and slow peeling rate was observed by scanning electron microscope imaging, elemental analysis, and contact angle measurement. A simple adhesion test was deployed in this work to introduce potential application of worm-like PDMS structures.

2. Experimental Section

2.1. Synthesis of the titania nanotubular template

Titania nanotubes array was synthesised by potentiostatic anodising of 0.25 mm thick titanium foil (99.5% metals basis purity, Alfa Aesar) in fluoride contained glycerol electrolyte [38]. The foil was cut into 4 cm x 1.5 cm and wet polished using distilled water with 320, 800, 1200, 4000 grades of SiC, respectively. These were followed by rinsing with water and acetone. Anodising was performed using a DC regulated power supply in a two-electrode configuration with titanium foil as anode and graphite as cathode at 1.2 cm separation. An

area of 2 cm x 1.5 cm of titanium foil was immersed in an electrolyte containing 0.25 wt.% NH_4F and 2 vol.% DI water in glycerol (≥98.5%, Sigma Aldrich). A constant voltage (60 V) was applied for 6 h anodising at 22±2.5^oC with a stirring speed of 150 rpm to synthesise a uniform titania nanotubular array. After anodising, samples were taken out, rinsed with ethanol, dried in a N_2 stream followed by bath ultrasonication in acetone for 1 min.

2.2. Silanisation of the titania nanotubes array

Titania nanotubes array were treated with fluoroalkyl silane solution to create self-assembled monolayer coating [39,40]. The nanotubes array were sequentially immersed for 1 h in methanol solution of 1.0 wt.% 1H,1H,2H,2H-perfluorooctyltrichloro silane (FOTS, Sigma Aldrich), rinsed with pure methanol and dried in N_2 stream. The array was subsequently heated in an oven at 140^oC for 1 h.

2.3. Moulding of polydimethylsiloxane

Several coated titania nanotubular templates were soaked in toluene for 10 min or directly deployed for PDMS moulding. Commercially available PDMS, Slygard 182 elastomer kit (Dow Corning) contains silicon elastomer base and curing agent. Both components were mixed in a ratio of 10 to 1 (elastomer base to curing agent). Toluene was added to dilute the mixture, creating either 50 vol.% or 33.33 vol.% of PDMS. 500 µL of the mixed solution was casted onto 2 cm x 1.5 cm of titania nanotubes array and left under vacuum for 4 h to remove solvent and gas from the pores of the nanotubes, which generated during curing of PDMS. 8.33 MPa of pressure were applied to some samples by hydraulic pressure. For pressurised samples, 500 µL of the PDMS mixture was added as the backing layer. All samples were cured in an oven at 140^oC for 20 min and carefully peeled off (≈1 mm s^{-1}) from the nanotubular template, except for sample 6 when rapid peeling (>3 mm s^{-1}) was conducted.

A control sample was made by casting 500 µL of 50 vol.% PDMS in toluene, on soda lime glass, followed by vacuum treatment for 4 h. It was cured at 140^{o}C for 20 min and peeled carefully. The process is illustrated in Figure 1 and the nomenclature of samples is provided in Table 1.

Figure 1

Table 1

2.4. Characterisation

The morphology of titania nanotubes and PDMS analysis were carried out by field emission scanning electron microscopy (FESEM, JEOL JSM 6500F) in which the elemental analysis was performed during energy dispersive X-ray spectroscopy (Oxford Inca system). To estimate the deviation of nanostructures morphology, 50 measurements were made on each sample in Microsoft Visio using the FESEM images. The cross section of titania nanotubes was inspected by peeling some of the nanotubes array using 3M scotch tape. PDMS samples were sputtered with thin layers of gold altering its surface conductivity for FESEM characterisation. To ensure the silanisation of TiO_2, Fourier transform infrared spectroscopy (FTIR) was deployed using Nicolet 380 FT-IR Spectrometer, Thermo Scientific. The contact angle of DI water on samples was measured using a drop shape analyser-DSA100. A droplet of deionized water (1 µL) was deposited on the sample surface using a syringe clamped on the column of the apparatus. The images were recorded with a charge-coupled device (CCD) camera and transmitted the information to the computer. DSA3 software was deployed to perform automatic calculation of contact angle for three measurements on each sample.

3. Results and Discussion

3.1. Fabrication of surface modified titania nanotubes template

The nanotubes length and diameter are essential as moulding template in which large nanotubes, up to 200 nm in diameter, can be produced by anodising [41]. Electrolyte composition, applied voltage, and duration of anodising exerted significant influence on nanotubes length and diameter. Anodising titanium foil in glycerol-based solution (0.25 wt.% NH_4F, 2 vol.% water in glycerol) at 60 V for 6 h formed a nanotubes array with 140±20 nm (Figure 2 a) and ≈1.5 μm (Figure 2 b) for diameter and length, respectively.

Figure 2

Figure 3

To facilitate separation of PDMS from the template, the nanotubular array was coated with fluoroalkyl chlorosilane to lower its surface energy and adhesion [42]. Perfluorooctyltrichloro silane (FOTS) was adsorbed and hydrated onto the surface of nanotubes. Figure 3 shows the FTIR spectra of anodised TiO_2 and silanised TiO_2. Both samples exhibited the characteristic of Ti-O and Ti-O-Ti peaks at 980 and 820 cm^{-1} [43]. Nevertheless, several changes in the FTIR peaks were observed after the silanisation. The -OH and H-O-H peaks of anodised TiO_2 were disappeared due to the reaction with silane group and transformation into hydrophobic nature. The attachment of fluoroalkyl silane groups was shown by Si-O-C, C-F, $-CH_2$ and $-CH_3$ peaks at 1145, 1250, ≈1600, and ≈2800 cm^{-1} [44]. Heat treatment at 140^{o}C for 1 h ensured condensation and polymerisation of self-assembled monolayer (SAM) coating on the surface. Helmy *et al.* [45] studied the effect of silane head groups on its attachment onto titania surface. SAMs from hydrolysis of FOTS were grafted significantly faster and denser than SAMs of triethoxy and dimethylchlorosilane as described by first order kinetics reaction. Although the combination of silane with various chain lengths was proven to yield

the highest hydrophobic properties, the increment was not significant which was 157.1° to 158.7° [46]. Here, only one silane (FOTS) was deployed to alter the surface of nanotubes presenting the cost-effective process of functionalisation. Contact angle measurements in Figure 2 c showed that the wetting properties of titania nanotubes array switched from hydrophilic (≈0°) to hydrophobic (128.7±4.5°). The hydrophobic nature of nanotubes after treatment implied adequate attachment of fluoroalkyl chlorosilane. The procedure improved the wetting of toluene and PDMS during the critical toluene soaking step.**3.2.**

Moulding of polydimethylsiloxane

In a vertical cylinder, it has been postulated that time required for liquid to penetrate the pore are proportional to the viscosity of the liquid, which can be described by Lucas-Washburn equations as [47]

$$t = X[-Yz - ln(1 - Yz)] \quad (1)$$

$$X = 16\mu\sigma cos\theta/\rho^2 g^2 r^3 \quad (2)$$

$$Y = \rho gr/2\sigma cos\theta \quad (3)$$

where *t* is the time required to fill the tube, ρ is the density difference between the penetrating liquid and the fluid (e.g., gas, other liquid) inside the porous medium, μ is dynamic viscosity of liquid, *z* is the depth of the tube, *r* is the radius of the tube, σ is surface tension at liquid/air interface, θ is contact angle of liquid. The addition of 60 wt.% toluene to the PDMS may reduce the viscosity of PDMS by 1 order magnitude [48]. For silicon nanoholes, the filling depth was increased exponentially by >40 wt.% addition of toluene [48]. Hence, the weight percentage of PDMS in toluene as well as the use of toluene soaking was studied in this work. The contact angle of the liquid was correlated with the wetting of the

nanotubular template. The states of wetting on rough/porous surfaces, which in this case the surface was patterned by nanotubular array, can be described by two states, Wenzel [49] and Cassie-Baxter [50] state. The Wenzel model is used for fully wetted surface when the liquid contacts the surface area of the sample without any gap. The Cassie-Baxter model is deployed when a sessile drop sits on the top of the surface while substances (e.g., gas or immiscible liquid) entrapped beneath the drop [51]. The Cassie-Baxter state only occurs when the value of the roughness is small enough compared to the size of the droplet.

Figure 4 a show a flat surface of PDMS which casted on soda lime glass without any treatment as sample 1 or the control sample. In sample 2, 3, and 4, the nanotubes were filled by toluene to the base of the tubes (Wenzel state) after soaking the nanotubular template in toluene for 10 minutes, which may ultimately enhance the surface wetting of the tube by PDMS [19]. However, only microroughness observed on diluted PDMS sample 2 and 3 (Figure 4 b & c) indicating improper infiltration of PDMS. More defined micro-bumps were observed in sample 3 (as shown in Figure 4 c and d) indicating deeper infiltration of 33.33 vol.% PDMS. Without stirring, toluene in nanotubes (from toluene soaking process) may not mixed well with PDMS at 25^{o}C and hold the PDMS mixture on top of the tube, in which external energy was needed to overcome the energy barrier of Cassie-Baxter state. Energy barrier increased as the diameter of tubes decreased which exerted significant effect on nanosized sample [52]. Additional pressure on the sample improved the infiltration of PDMS. Figure 4 e & f showed bumps from PDMS sagging.

Figure 4

3.3. Hydraulic pressing

After hydraulic pressing, the filling depth of PDMS was 221.64±52.76 nm in sample 4 (Figure 5 a), which far less than the length of nanotubes (≈1500 nm). Toluene left inside the nanotubes after toluene soaking impeded further infiltration of PDMS. The removal of toluene soaking in sample 5 may increase probability of trapped air inside nanotubes. Conversely, air is more compressible compared to liquid toluene during hydraulic pressing because air is a mixture of gases. For air, the pressure needed for filling the nanotubes was only around 0.101 MPa, which can be calculated by following equation.

$$P = P_{air} + P_{PDMS} \quad (4)$$

$$P_{PDMS} = \rho g h \quad (5)$$

Where P is total pressure required, P_{air} is atmospheric pressure (0.101 MPa), ρ is the density of Slygard 182, which is 1049.97 kg m^{-3}, and g is gravity (9.81 N kg^{-1}), while h is the depth of the tube, 1.5 x 10^{-6} m. Since the pores are parallel, the pressure needed to fill all the pores was the same, around 0.101 MPa. However, 8.33 MPa of pressure was applied to overcome the wall friction or debris that might hampered the penetration.

The filling depth was increased by this method (Figure 5 b & c). The height of worm-like PDMS were similar to the nanotube length in which the average length of worm-like PDMS were 1172±193 nm. The length frequency histograms of sample 4 and 5 were provided in Figure 6. Although the sample 5 had a significantly longer length (i.e., 1.17 micron) compared to sample 4 (221±52.76 nm), the sample 5 was broadly distributed with the deviation of 193 nm. PDMS may swell during the moulding process due to crosslinking of PDMS, yielding larger PDMS diameter (≈200 nm) compared to titania mould (≈140 nm). This result was in accordance with the swelling study conducted by Vogt *et al.* where the PDMS was swollen by around 30% for a 10:1 wt.% base to curing agent ratio of PDMS [53].

The peeling rate was important in ensuring complete separation of PDMS and nanotubes. The peeling rate was ≈1 mm s^{-1} for sample 2, 3, 4, and 5. In Figure 5 e and f, rapid peeling rate (approx. >3 mm s^{-1}) on sample 6 produced either flat PDMS or composites of PDMS and TiO_2 nanotubes. The presence of TiO_2 was proven by energy dispersive X-ray (EDX) spectroscopy, where the Ti atoms were absence in Figure 5d yet appeared in Figure 5f. The swollen PDMS in TiO_2 nanotubes exhibited mechanical interlocking between PDMS nanostructures and inner wall of nanotubes hampering the detachment of PDMS structures.

Figure 5

Figure 6

Contact angle measurement in Figure 7 a & b showed enhancement from 100.3±1.2° to 109.6±1.1° for flat and patterned PDMS sample 5, respectively due to the improvement in the surface roughness. When tilted up to around 45°, the 1 µL water droplet remained pinned to the surface rather than rolled over it, indicating a Wenzel state of wetting. It was expected that the Wenzel state would be the stable wetting state of rough PDMS in which the transition to Wenzel state occurred at a Wenzel limit of 110° [54]. Ground collapse and collision of PDMS may diminished the roughness of sub-micron textured on PDMS sample. Ground collapse and collision of PDMS can be attributed to low modulus of soft PDMS (7.3 MPa for Sylgard 182) [37] and adhesive force to the ground (base of PDMS) [55]. The critical aspect ratio of PDMS to avoid collapses are around 2, for tube diameter less than 500 nm [56]. Such collapse was expected in this work considering high aspect ratio of PDMS (≈6). Stiffer materials such as epoxy and polyurethane can be used to prevent collapsing. Collapses of worm-like PDMS can be recovered to upright position by ultrasonication in low surface

energy solution [57]. However, high aspect ratio worm-like PDMS are metastable and easily disturbed by moisture or electron beam during SEM characterisation [55].

Figure 7

3.4. Adhesive strength

PDMS nanostructures can be used in climbing robots [58], microfluidics [59], and dry dermal patch [11] devices. Here, an adhesion test was conducted to stimulate potential application as dry adhesive. The experimental setup was outlined in Figure 8.

Figure 8

A PDMS of 1 cm^2 area was attached to the pin using carbon tape. The patterned surface of PDMS was then pressed on the planar glass surface with prior cleaning by acetone. The glass, PDMS, and pin setup was positioned vertically. The weighing scale was hung on the tip of the pin. Silica powder was added gradually until the adhesive was peeled off from the glass. The peeling force was calculated from the final mass. Hence, the shear adhesive strength can be obtained as N cm^{-2}. The adhesive strength of sample 3, 4, 5 were 0.009, 0.312, 0.29 N cm^{-2} while all the other samples were too weak to be measured. A significant increase was seen on the hydraulic pressed sample (sample 4 and 5) compared to non-pressed sample (sample 3).

The adhesion mechanism of dry adhesive has been extensively studied to explain the adhesion mechanism used in gecko attachment to solid surfaces. It was found that the dry adhesion mainly relies on van der Waals forces rather than electrostatic or suction [60]. Small and dense nanostructures (i.e., 14400 setae per mm^2 in gecko) resulted in high adhesion energy from van der Waals forces. Sample 4 and 5 in this work exhibited a dense worm-like

PDMS (≈9 worm-like structures per μm^2) compared to sample 3 with approximately 3 bumps per μm^2 as determined by SEM. Although the aspect ratio in sample 5 was higher than sample 4, the structures were collapsed to the ground hence the effective height was only the diameter of the worm-like structure producing less adhesive energy compared to sample 4. The 0.312 N cm^2 adhesion strength of sample 4 was comparable to fibrin glue that is ≈0.2–0.5 N cm^2, which could be useful for medical dry adhesive [61].

4. Conclusions

Titania nanotubular array, created by anodising titanium foil at 60 V using 0.25 wt.% NH_4F and 2 vol.% water in glycerol as electrolyte, has been used as a template for PDMS (Sylgard 182) moulding. It was found that application of hydraulic pressure during casting PDMS into TiO_2 nanotubes array mould has significantly improved the infiltration of the polymer into the pores of nanotubes. Although toluene soaking is commonly used in the moulding protocol to improve template wetting, it probably hindered full penetration of PDMS during hydraulic pressing. Complete penetration of PDMS mixture was observed on the hydraulic pressed sample without toluene soaking. The curing of PDMS mixture inside the pores of the tubular array followed by peeling of the polymer film has resulted in formation of worm-like structure with typical diameter ≈200 nm and length ≈1.17 µm. However, obtained high aspect ratio worm-like PDMS structures were deformed and collapsed due to low modulus of soft PDMS. The resulting structure was used as a dry adhesive, resulting in an adhesive strength up to 0.312 N cm^2.

Abbreviations

PDMS, polydimethylsiloxane; TiO_2, titanium dioxide; FOTS, 1H,1H,2H,2H-perfluorooctyltrichloro silane.

Acknowledgments

This project is supported financially by Indonesian Endowment Fund for Education (LPDP) and Erasmus+ scholarship.

References

1. Xia, Y.; Whitesides, G. M. *Angew. Chemie Int. Ed.* **1998**, *37*, 550.

2. ElMahmoudy, M.; Curto, V. F.; Ferro, M.; Hama, A.; Malliaras, G. G.; O'Connor, R. P.; Sanaur, S. *J. Appl. Polym. Sci.* **2019**, *136*, 47029.

3. Xu, H.; Gomez-Casado, A.; Liu, Z.; Reinhoudt, D. N.; Lammertink, R. G. H.; Huskens, J. *Langmuir* **2009**, *25*, 13972.

4. Lee, D.-H.; Jung, S.-H.; Kwon, O. J.; Kim, M.-S.; Park, J.-S.; Lee, E.; Jung, B. J.; O, B.-H.; Park, S.-G.; Lee, J.-K. *J. Appl. Polym. Sci.* **2017**, *134*, 45184.

5. Yuan, L.; Wang, Z.; Li, Y.; Wu, T. *J. Appl. Polym. Sci.* **2019**, *136*, 47296.

6. Raj M, K.; Chakraborty, S. *J. Appl. Polym. Sci.* **2020**, 48958.

7. McDonald, J. C.; Whitesides, G. M. *Acc. Chem. Res.* **2002**, *35*, 491.

8. Ong, J. K. Y.; Moore, D.; Kane, J.; Saraf, R. F. *ACS Appl. Mater. Interfaces* **2014**, *6*, 14278.

9. Bucknall, D. G. *Nanolithography and Patterning Techniques in Microelectronics*; Elsevier, **2005**.

10. Chuah, Y. J.; Koh, Y. T.; Lim, K.; Menon, N. V.; Wu, Y.; Kang, Y. *Sci. Rep.* **2015**, *5*, 1.

11. Harito, C.; Utari, L.; Putra, B. R.; Yuliarto, B.; Purwanto, S.; Zaidi, S. Z. J.; Bavykin, D. V.;

Marken, F.; Walsh, F. C. *J. Electrochem. Soc.* **2020**, *167*, 037566.

12. Yabu, H.; Saito, Y.; Nakamichi, Y.; Hirai, Y.; Fujinami, S.; Nakajima, K.; Nishi, T.; Shimomura, M. *Polym. J.* **2012**, *44*, 573.

13. Sun, M.; Luo, C.; Xu, L.; Ji, H.; Ouyang, Q.; Yu, D.; Chen, Y. *Langmuir* **2005**, *21*, 8978.

14. Zhang, B.; Luo, Y.; Pearlstein, A. J.; Aplin, J.; Liu, Y.; Bauchan, G. R.; Payne, G. F.; Wang, Q.; Nou, X.; Millner, P. D. *ACS Appl. Mater. Interfaces* **2014**, *6*, 12467.

15. Wu, W.; Guijt, R. M.; Silina, Y. E.; Koch, M.; Manz, A. *RSC Adv.* **2016**, *6*, 22469.

16. Pan, J.; Chen, H.; Zhang, D.; Zhang, X.; Yuan, L.; Aobo, L. *J. Micromechanics Microengineering* **2013**, *23*, 075018.

17. Mishra, H.; Schrader, A. M.; Lee, D. W.; Gallo, A.; Chen, S.-Y.; Kaufman, Y.; Das, S.; Israelachvili, J. N. *ACS Appl. Mater. Interfaces* **2016**, *8*, 8168.

18. Lee, C. J.; Blumenkranz, M. S.; Fishman, H. A.; Bent, S. F. *Langmuir* **2004**, *20*, 4155.

19. Con, C.; Cui, B. *Nanoscale Res. Lett.* **2013**, *8*, 394.

20. Jenkins, G. In *Microfluidic Diagnostics*; Humana Press: New Jersey, **2013**; pp 153.

21. Migliaccio, C. P.; Lazarus, N. *Appl. Surf. Sci.* **2015**, *353*, 269.

22. Zhang, E.; Liu, Y.; Yu, J.; Lv, T.; Li, L. *J. Mater. Chem. B* **2015**, *3*, 6571.

23. Ting, Y.-C.; Shy, S.-L. In *Alternative Lithographic Technologies IV*; Tong, W. M., Ed.; International Society for Optics and Photonics: San Jose, **2012**; pp 83232H.

24. Zhou, W.; Zhang, J.; Li, X.; Liu, Y.; Min, G.; Song, Z.; Zhang, J. *Appl. Surf. Sci.* **2009**, *255*, 8019.

25. Zhou, W.; Niu, X.; Min, G.; Song, Z.; Zhang, J.; Liu, Y.; Li, X.; Zhang, J.; Feng, S. *Microelectron. Eng.* **2009**, *86*, 2375.

26. Park, O.-H.; Cheng, J. Y.; Hart, M.; Topuria, T.; Rice, P. M.; Krupp, L. E.; Miller, R. D.; Ito, H.; Kim, H.-C. *Adv. Mater.* **2008**, *20*, 738.

27. Davis, J. R. *Metals Handbook Desk Edition*; 2nd ed.; ASM International, **1998**.

28. Caldona, E. B.; Albayalde, J. M. C.; Aglosolos, A. M. P.; Bautista, K. S.; Tavora, M. D.; Cabalza, S. A. P.; Diaz, J. R. O.; Mulato, M. D. *J. Polym. Environ.* **2019**, *27*, 1564.

29. Barman, J.; Majumder, S. K.; Roy, P. K.; Khare, K. *RSC Adv.* **2018**, *8*, 13253.

30. Odom, T. W.; Love, J. C.; Wolfe, D. B.; Paul, K. E.; Whitesides, G. M. *Langmuir* **2002**, *18*, 5314.

31. Harito, C.; Porras, R.; Bavykin, D. V.; Walsh, F. C. *J. Appl. Polym. Sci.* **2017**, *134*, 1.

32. Putra, B. R.; Harito, C.; Bavykin, D. V.; Walsh, F. C.; Wahyuni, W. T.; Boswell, J. A.; Squires, A. M.; Schmitt, J. M. F. F.; Da Silva, M. A.; Edler, K. J.; Fletcher, P. J.; Gesell, A. E.; Marken, F. *J. Solid State Electrochem.* **2019**, *23*, 1237.

33. Gong, D.; Grimes, C. A.; Varghese, O. K.; Hu, W.; Singh, R. S.; Chen, Z.; Dickey, E. C. *J. Mater. Res.* **2001**, *16*, 3331.

34. Macak, J. M.; Tsuchiya, H.; Taveira, L.; Aldabergerova, S.; Schmuki, P. *Angew. Chemie Int. Ed.* **2005**, *44*, 7463.

35. Prakasam, H. E.; Shankar, K.; Paulose, M.; Varghese, O. K.; Grimes, C. A. *J. Phys. Chem. C* **2007**, *111*, 7235.

36. Macak, J. M.; Hildebrand, H.; Marten-Jahns, U.; Schmuki, P. *J. Electroanal. Chem.*

2008, *621*, 254.

37. SYLGARD® 182 SILICONE ELASTOMER KIT. *Dow corning Corp.* http://www.dowcorning.com/applications/search/default.aspx?R=130EN (accessed August 10, 2017).

38. Martins, A. S.; Harito, C.; Bavykin, D. V.; Walsh, F. C.; V. Lanza, M. R.; V Lanza, M. R. *J. Mater. Chem. C* **2017**, *5*, 3955.

39. Hu, Z.; Zhang, X.; Liu, Z.; Huo, K.; Chu, P. K.; Zhai, J.; Jiang, L. *Adv. Funct. Mater.* **2014**, *24*, 6381.

40. Kim, H.; Noh, K.; Choi, C.; Khamwannah, J.; Villwock, D.; Jin, S. *Langmuir* **2011**, *27*, 10191.

41. Bavykin, D. V.; Walsh, F. C. *Titanate and Titania Nanotubes*; Royal Society of Chemistry: Cambridge, **2009**.

42. Chen, J.-K.; Ko, F.-H.; Hsieh, K.-F.; Chou, C.-T.; Chang, F.-C. *J. Vac. Sci. Technol. B Microelectron. Nanom. Struct.* **2004**, *22*, 3233.

43. Patel, S. B.; Baker, N.; Marques, I.; Hamlekhan, A.; Mathew, M. T.; Takoudis, C.; Friedrich, C.; Sukotjo, C.; Shokuhfar, T. *RSC Adv.* **2017**, *7*, 30397.

44. Brassard, J. D.; Sarkar, D. K.; Perron, J. *ACS Appl. Mater. Interfaces* **2011**, *3*, 3583.

45. Helmy, R.; Fadeev, A. Y. *Langmuir* **2002**, *18*, 8924.

46. Spataru, C. I.; Purcar, V.; Ghiurea, M.; Somoghi, R.; Donescu, D. *J. Optoelectron. Adv. Mater.* **2013**, *15*, 1438.

47. Marmur, A. *Langmuir* **2003**, *19*, 5956.

48. Koo, N.; Bender, M.; Plachetka, U.; Fuchs, A.; Wahlbrink, T.; Bolten, J.; Kurz, H. *Microelectron. Eng.* **2007**, *84*, 904.

49. Wenzel, R. N. *Ind. Eng. Chem.* **1936**, *28*, 988.

50. Cassie, A. B. D.; Baxter, S. *Trans. Faraday Soc.* **1944**, *40*, 546.

51. Giljean, S.; Bigerelle, M.; Anselme, K.; Haidara, H. *Appl. Surf. Sci.* **2011**, *257*, 9631.

52. Murakami, D.; Jinnai, H.; Takahara, A. *Langmuir* **2014**, *30*, 2061.

53. Qiang, Z.; Zhang, Y.; Groff, J. A.; Cavicchi, K. A.; Vogt, B. D. *Soft Matter* **2014**, *10*, 6068.

54. Mishra, H.; Schrader, A. M.; Lee, D. W.; Gallo, A.; Chen, S. Y.; Kaufman, Y.; Das, S.; Israelachvili, J. N. *ACS Appl. Mater. Interfaces* **2016**, *8*, 8168.

55. Zhang, Y.; Lo, C.-W.; Taylor, J. A.; Yang, S. *Langmuir* **2006**, *22*, 8595.

56. Roca-Cusachs, P.; Rico, F.; Martínez, E.; Toset, J.; Farré, R.; Navajas, D. *Langmuir* **2005**, *21*, 5542.

57. Liu, H.; Lei, B.; Jiang, W.; Li, Y.; Yin, L.; Chen, B.; Shi, Y. *RSC Adv.* **2016**, *6*, 16640.

58. Dharmawan, A. G.; Xavier, P.; Anderson, D.; Perez, K. B.; Hariri, H. H.; Soh, G. S.; Baji, A.; Bouffanais, R.; Foong, S.; Low, H. Y.; Wood, K. L. In *Proceedings of the ASME Design Engineering Technical Conference*; American Society of Mechanical Engineers (ASME), **2018**; Vol. 5B-2018.

59. Atakan, H. B.; Ayhan, F.; Gijs, M. A. M. *Lab Chip* **2020**, *20*, 155.

60. Autumn, K.; Sitti, M.; Liang, Y. A.; Peattie, A. M.; Hansen, W. R.; Sponberg, S.; Kenny, T. W.; Fearing, R.; Israelachvili, J. N.; Full, R. J. *Proc. Natl. Acad. Sci. U. S. A.* **2002**, *99*, 12252.

61. Düregger, K.; Frenzel, S.; Eblenkamp, M. *Curr. Dir. Biomed. Eng.* **2017**, *3*, 397.

Table Caption

Table 1. Nomenclature of samples

Table 1

Sample	Name	Description
1	Flat	Control sample casted on soda lime glass
2	TS-0.5P-NP	Soaked with toluene, 50 vol.% PDMS, no pressing
3	TS-0.3P-NP	Soaked with toluene, 33.33 vol.% PDMS, no pressing
4	TS-0.3P-P	Soaked with toluene, 33.33 vol.% PDMS, hydraulic pressing
5	NTS-0.3P-P	Not soaked with toluene, 33.33 vol.% PDMS, hydraulic pressing
6	NTS-0.3P-P-R	Rapid peeling sample, not soaked with toluene, 33.33 vol.% PDMS, hydraulic pressing

Figure Captions

Figure 1. The illustration of PDMS moulding with titania nanotubes array.

Figure 2. SEM images of (a) top view of titania nanotubular array, (b) cross-section of nanotubes, and contact angle measurement of (c) uncoated nanotubular array, (d) coated nanotubular array

Figure 3. FTIR spectra of (i) the as-anodised TiO_2 nanotubular array, (ii) the silanised TiO_2

Figure 4. SEM images of PDMS, (a) control sample 1, (b) sample 2 TS-0.5P-NP, (c) sample 3 TS-0.3P-NP, (d) magnified image of sample 3, (e) sample 4 TS-0.3P-P, (f) magnified and 30^o tilted image of sample 4

Figure 5. SEM images of PDMS, (a) 30^o tilted images of sample 4 TS-0.3P-P (b) top view of sample 5 NTS-0.3P-P, (c) magnified images of sample 5 viewed on top, (d) EDX spectra of sample 5, (e) rapid peeling on sample 6 NTS-0.3P-P-R, (f) EDX spectra of sample 6

Figure 6. Length frequency histogram of (a) PDMS sample 4, (b) PDMS sample 5

Figure 7. Contact angle measurement of (a) flat PDMS sample, (b) sample 5 patterned PDMS

Figure 8. Simple experimental setup to measure dry adhesive strength, (a) the attachment of PDMS to pin holder, (b) the measurement of adhesive force on glass by weight addition

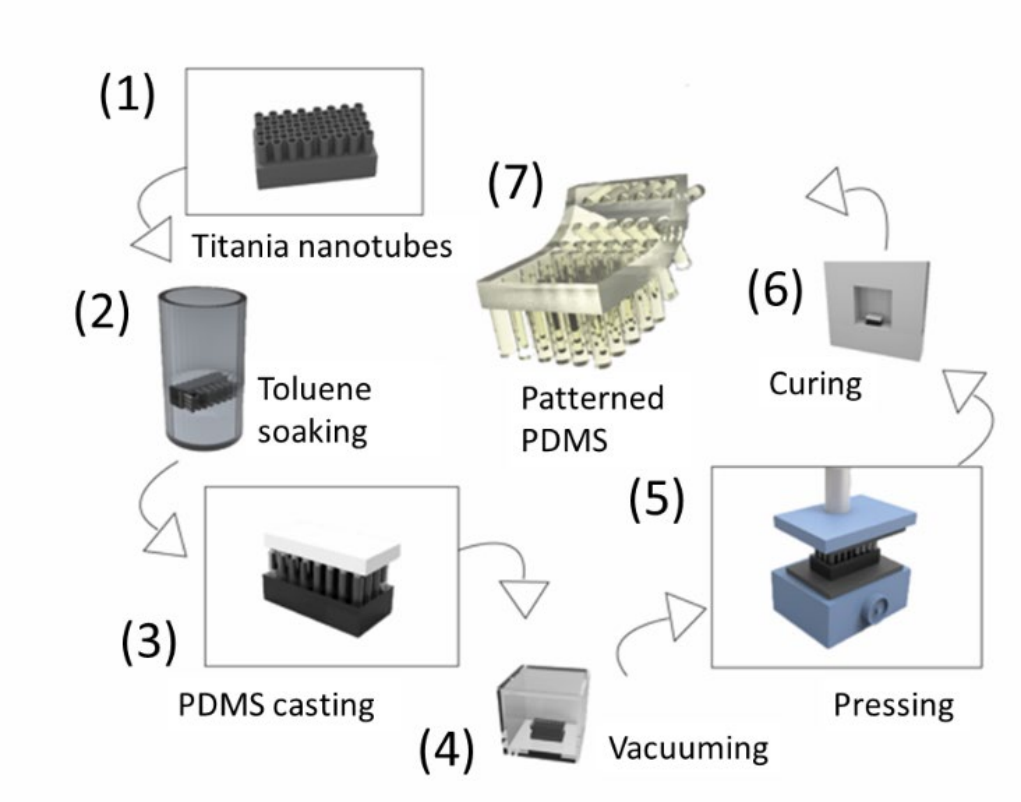
(1)
Titania nanotubes
(2)
Toluene
soaking
(3)
PDMS casting
(4)
Vacuuming
(5)
Pressing
(6)
Curing
(7)
Patterned
PDMS

Figure 1

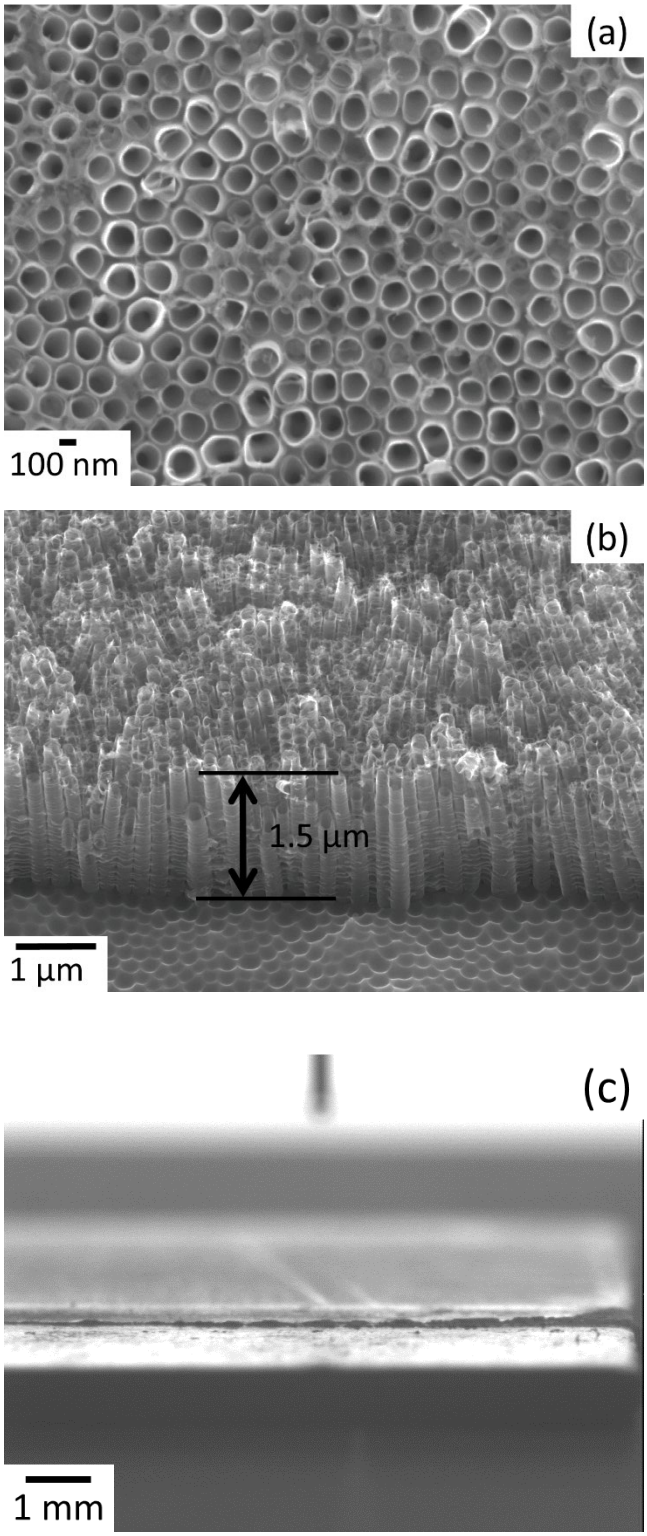
(a)
100 nm
(b)
1.5 µm
1 µm
(c)
1 mm

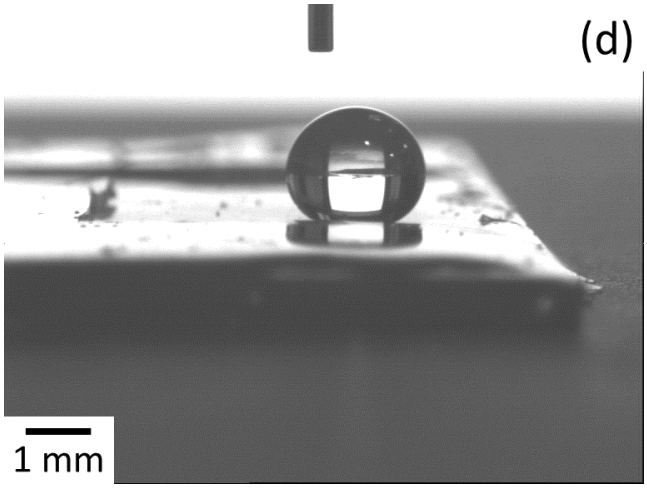

Figure 2

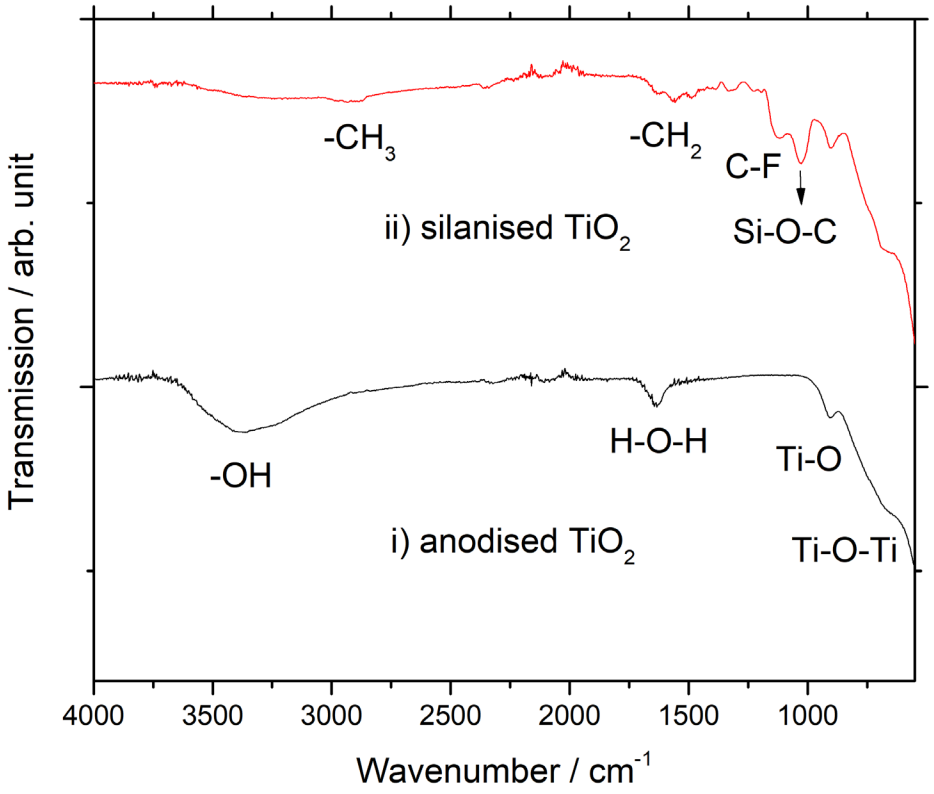
Transmission / arb. unit
-CH3
-CH2
C-F
Si-O-C
ii) silanised TiO2
-OH
H-O-H
Ti-O
Ti-O-Ti
i) anodised TiO2
4000
3500
3000
2500
2000
1500
1000
Wavenumber / cm-1

Figure 3

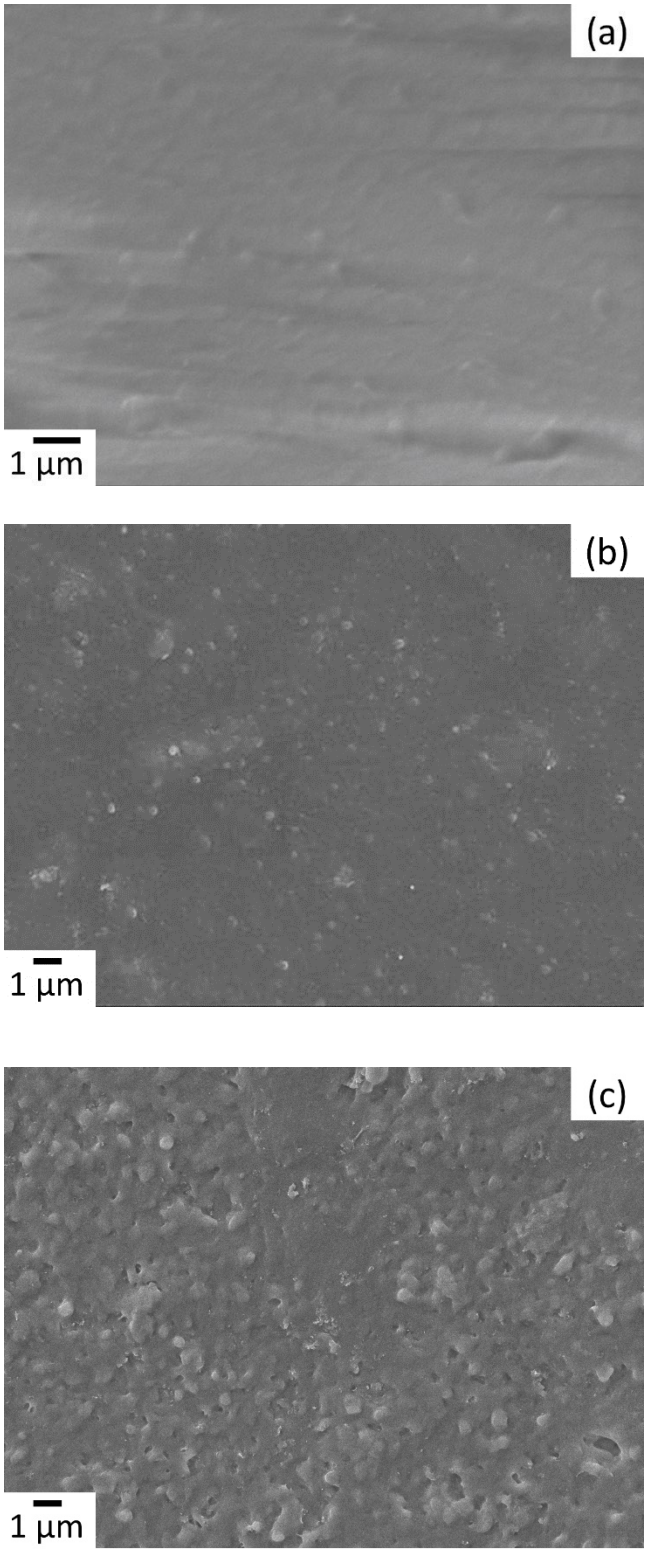
(a)
1 µm
(b)
1 µm
(c)
1 µm

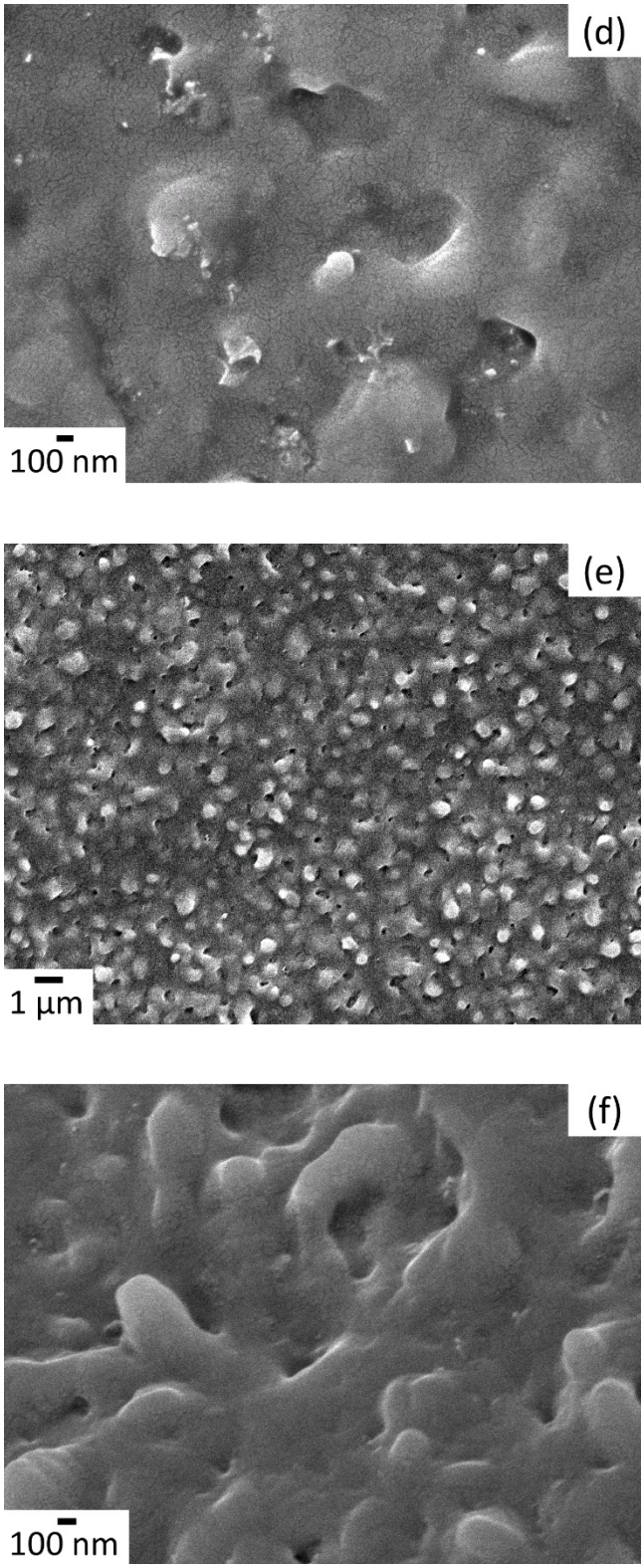

Figure 4

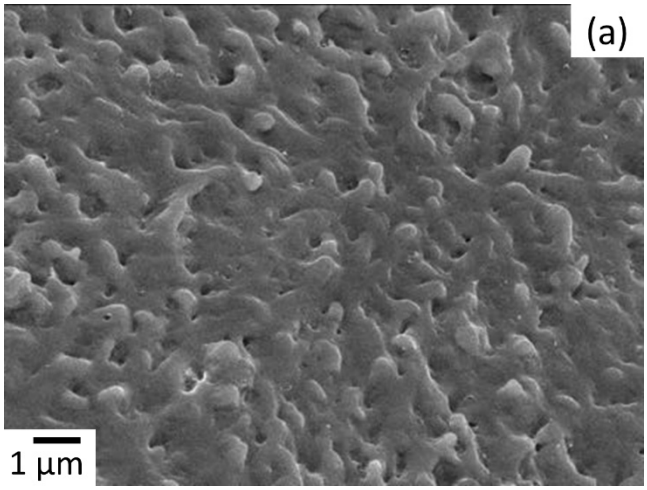
(a)
1 µm

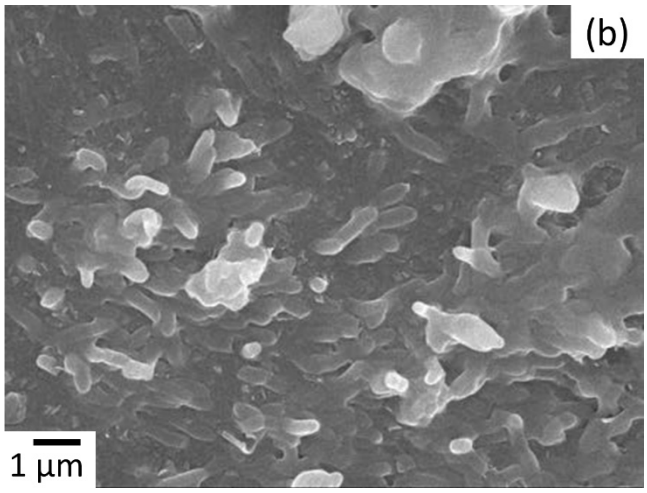
(b)
1 µm

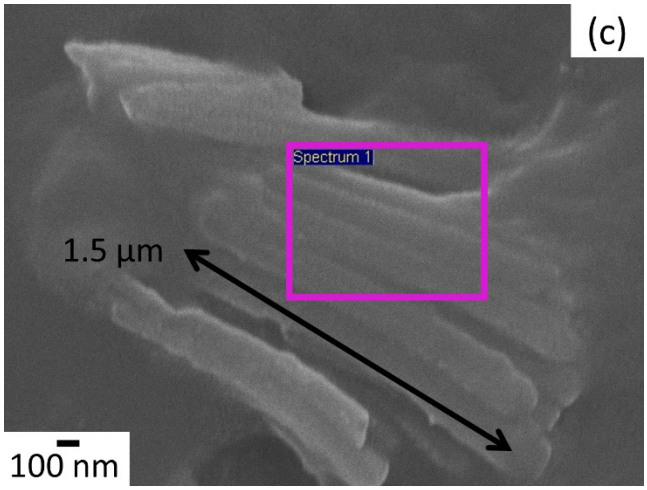
(c)
Spectrum 1
1.5 µm
100 nm

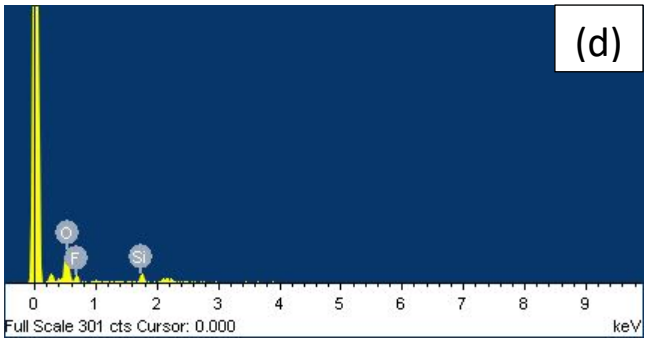
(d)
O
F
Si
0 1 2 3 4 5 6 7 8 9
Full Scale 301 cts Cursor: 0.000
keV

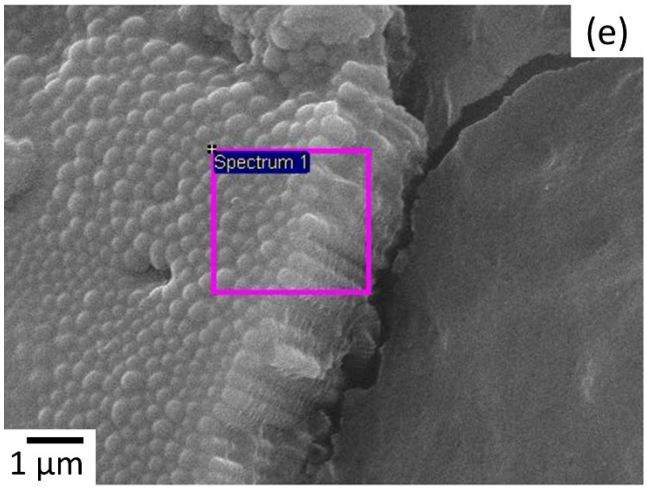
(e)
Spectrum 1
1 µm

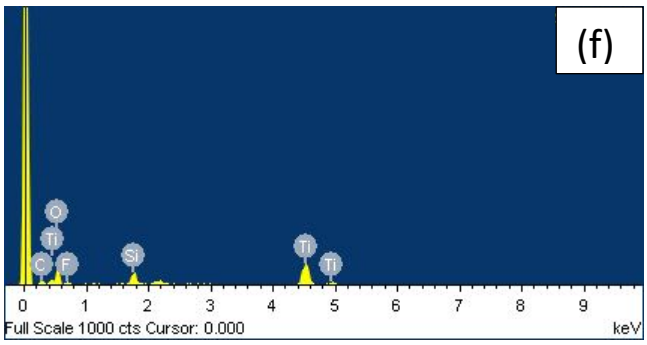
(f)
O
Ti
C
F
Si
Ti
Ti
0 1 2 3 4 5 6 7 8 9
Full Scale 1000 cts Cursor: 0.000
keV

Figure 5

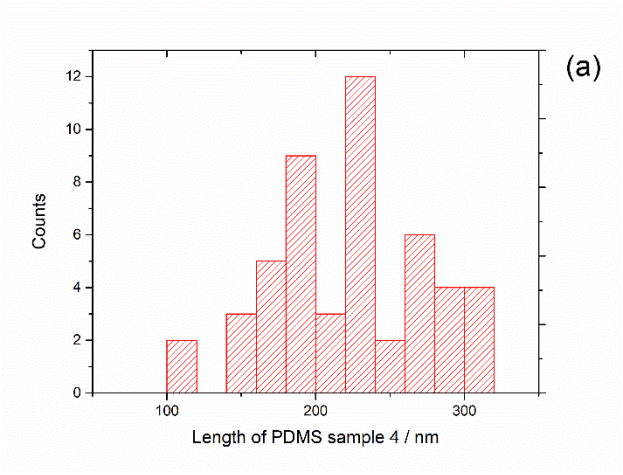
(a)
Counts
0
2
4
6
8
10
12
100
200
300
Length of PDMS sample 4 / nm

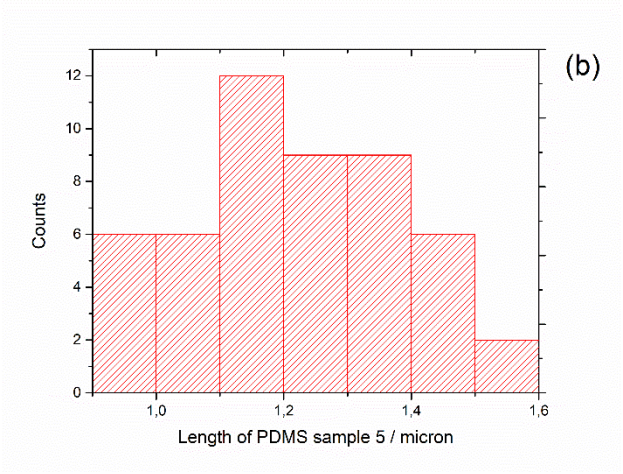
(b)
Counts
0
2
4
6
8
10
12
1,0
1,2
1,4
1,6
Length of PDMS sample 5 / micron

Figure 6

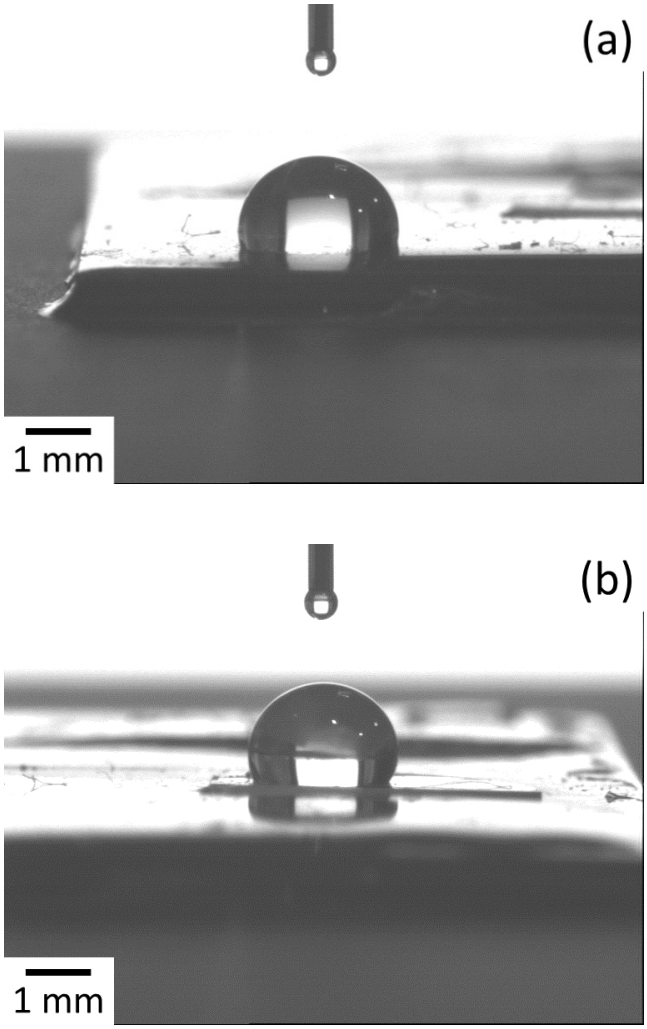

Figure 7

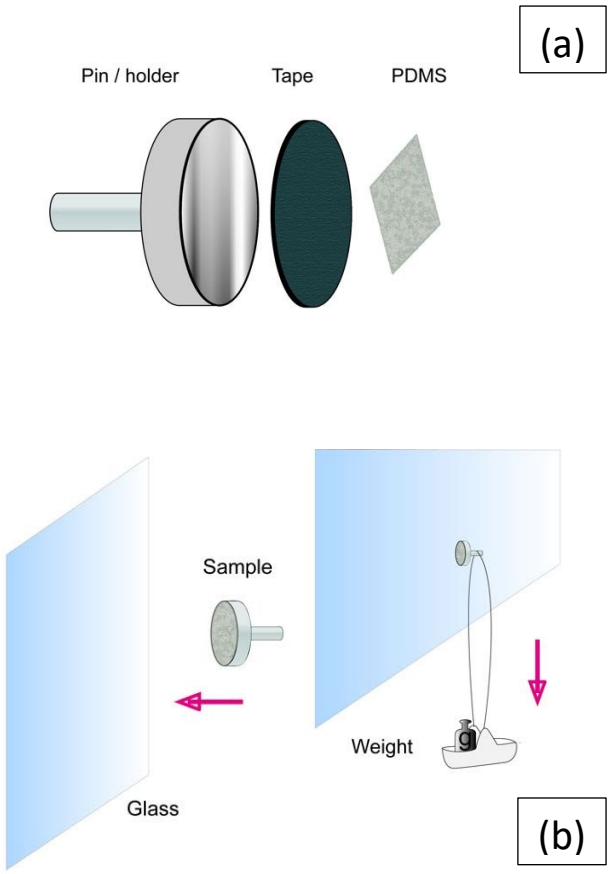

Figure 8